Seismic reservoir and source-rock analysis using inverse rock-physics modeling: A Norwegian Sea demonstration

Kenneth Bredesen[1], Erling Hugo Jensen[1, 2], Tor Arne Johansen[1, 2], and Per Avseth[3, 4]

Abstract

Identifying type of rocks and fluids from seismic-amplitude anomalies can be challenging because of seismic nonuniqueness and rock-physics ambiguities. Lithology and fluid predictions based on seismic properties therefore are often associated with uncertainties. On the Norwegian Shelf, clay-rich source rocks and hydrocarbon-filled sandstones often show similar AVO responses. A seismic screening method based on rock physics enables one to better discriminate between these different facies. This technique is demonstrated on seismic AVO data (i.e., acoustic impedance [AI] and V_P/V_S) from the Norwegian Sea. Rock-physics models for organic-rich shales and gas sandstones are calibrated using nearby well data. Then these models are used for predictions of rock parameters away from well locations. From these predictions, the likelihood of presence of organic-rich shales versus gas sandstones can be evaluated, based on a rock-physics approach. However, there are many uncertainties in the accuracy of the calibrated models and the seismic image of the target area. Hence, predictions should be evaluated along with other geologic and geophysical information before firm conclusions about these anomalies are made.

Introduction

The Upper Jurassic stratigraphy on the Norwegian Shelf is receiving increasing attention as prospectivity mapping of older (Middle Jurassic to Triassic) structural highs is becoming very mature, with few major discoveries made in recent years. The Upper Jurassic interval comprises the famous Kimmeridge Shale, which is the main source rock in the North Sea (Draupne Formation) and Norwegian Sea (Spekk Formation). However, the Upper Jurassic also includes some of the more promising new discoveries (e.g., the Sverdrup field in the North Sea in 2011 and the Pil discovery in the Norwegian Sea in 2014) on the Norwegian Shelf, representing reservoir sands that have been eroded from structural highs and redeposited downflank, later becoming traps for migrating hydrocarbons.

Several recent wells on the Norwegian shelf targeting Upper Jurassic traps did not encounter reservoir sands but only thick, organic-rich shales in the target interval. One of the key challenges is to distinguish high-porosity clean sandstones and organic-rich shales, which can have similar seismic signatures (e.g., Avseth et al., 2014).

The rock-physics properties of sandstones are well understood, and normal shales are well sampled in many wells. Organic-rich shales, however, can be complex. They are often condensed in wells located on structural highs, and there are still very few laboratory measurements done on these rocks, particularly on clay-rich source rocks such as the Kimmeridge Shale. These rocks can have a large variety in mineral compositions and total organic content.

Furthermore, both diagenesis and maturity level will change with burial. Pore-fluid type and saturation will change with maturation, and anisotropy will vary with clay content and compaction. All these effects will result in a wide range of possible seismic properties.

Figure 1 show crossplots of acoustic impedance (AI) and P-to-S velocity ratio (V_P/V_S) from well-log data (dot symbols) and seismic-inversion data (square symbols) from selected wells that penetrate gas sandstones (yellow) and organic-rich shales (blue). Along with the data, we have projected rock-physics templates (RPT), including models for organic-rich shales (red trend) and gas- and brine-saturated sandstones (white and black trends, respectively). The models are described and used later in this article.

The red arrow in Figure 1 indicates how seismic properties vary with kerogen maturation, in which hydrocarbons are first generated and later expelled. The seismic properties of organic-rich shales vary significantly and can overlap sandstones, making it difficult to differentiate them, especially from seismic-inversion data only. Hence, improved methods are required to better identify and discriminate these rocks from one another.

Various strategies concerning seismic screening for source rocks have been proposed. For example, Løseth et al. (2011)

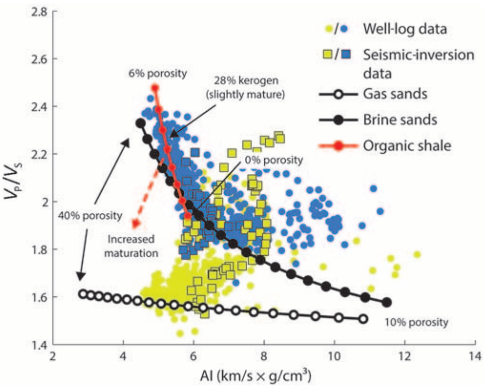

Figure 1. Rock-physics template analysis with seismic inversion and well-log data from the Norwegian Sea superimposed by templates of rock-physics models for organic-rich shales and gas- and water-saturated sandstones. The organic-rich shale is specified with 28% kerogen content, which is somewhat mature. Increased maturation and hydrocarbon expulsion imply decreasing AI and V_P/V_S, as illustrated by the red arrow.

[1]University of Bergen.
[2]Rock Physics Technology.
[3]Tullow Oil.
[4]Norwegian University of Science and Technology.

http://dx.doi.org/10.1190/tle34111350.1.

identify and characterize organic-rich shales from prestack seismic data based on the criteria that they exhibit relatively low acoustic impedance in combination with AVO Class IV signatures. Khadeeva and Vernik (2014) combine shear impedance with acoustic-impedance data to map total organic content (TOC) and presence of gas in organic-rich shales.

Avseth et al. (2014) compare well-log data of organic-rich shales of Upper Jurassic age with reservoir sands of Middle to Upper Jurassic age in rock-physics templates of acoustic impedance versus V_P/V_S and find that immature organic-rich shales have overlapping properties with brine-saturated sandstones but not with hydrocarbon-filled sandstones. Based on their analysis, some of the intrawell anomalies seen in the area of study could represent either mature source rocks or hydrocarbon-filled sandstones. However, in the lack of calibrated rock-physics models for the organic-rich shales, the analysis of Avseth et al. (2014) is inconclusive.

In our study, we want to evaluate the possibility of reservoir sands versus the presence of organic-rich shales using the same seismic inversion data from the Norwegian Sea as used by Avseth et al. (2014). We further investigate the intrawell anomalies and attempt to find out whether these represent organic-rich shales or potential reservoir sands. Rock-physics models from the literature are calibrated locally to log data from two neighboring wells. One well penetrates an organic-rich shale formation, and the other goes through gas sandstones.

For the modeling, we use the inverse rock-physics modeling (IRPM) of Johansen et al. (2013). This approach allows us to test various rock-physics models and evaluate the nonuniqueness of solutions. To better compare the performance of the two rock-physics models for the different geologic scenarios, we use an extension to the IRPM which gives us the possibility to compare the probability associated with the various predictions.

Inverse rock-physics modeling for distinguishing source rocks from reservoir

We use an extended version of the inverse rock-physics modeling of Johansen et al. (2013) to distinguish rocks. It associates model probabilities with the predictions, which relates how well the input data match the rock-physics model for a particular prediction of rock properties. The IRPM does an exhaustive search for possible matches between the input data and predicted rock properties. The search is done in forward-modeled so-called constraint cubes (Johansen et al., 2013) relating rock parameters to seismic parameters.

Figures 2a and 2b show constraint cubes for acoustic impedance and V_P/V_S, respectively, based on the gas-sandstone rock-physics model described in the next section. Figure 2c show all possible solutions of porosity, clay content (lithology), and gas saturation for one set of corresponding values of AI and V_P/V_S in the constraint cubes and associated model probabilities, as explained below.

In the extension to the IRPM which we use in this study, we specify probability density functions (PDF) for some of the reservoir parameters rather than static values, as used previously in IRPM. We then perform a Monte Carlo simulation in the forward modeling, resulting in not only single constraint cubes for the various seismic parameters but as many cubes as we have iterations in the simulation. Then a representative cube can be generated by calculating a mean value and the standard deviation for each node in the cubes.

Furthermore, PDFs also are specified for the input data, e.g., based on provided uncertainties for them. Then for each identified solution in the IRPM, it is possible to calculate a model probability based on how well the model fits the data, given the provided uncertainties. This model probability can be used to calculate weighted means and standard deviations of the predicted rock properties.

Furthermore, we define various facies; e.g., a gas sandstone can be specified to be highly porous, with little clay content and high gas saturation. The model probability then can be used to evaluate whether our model gives a good match with the input data for a given facies and how this compares to the other facies predictions. We refer to this as a facies identifier

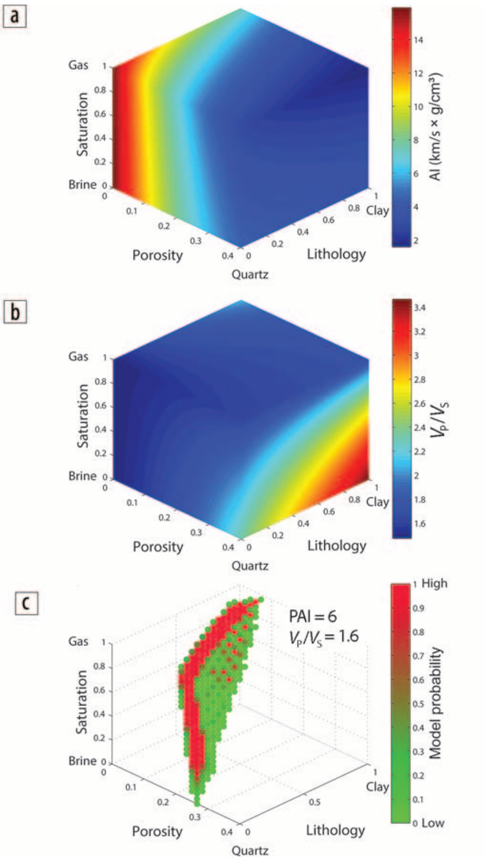

Figure 2. Forward-modeled rock-physics constraint cubes for (a) acoustic impedance (AI) and (b) V_P/V_S. (c) Corresponding solutions for AI = 6 km/s × g/cm³ and V_P/V_S = 1.6 km/s × g/cm³, where the color scale denotes model probability.

that has a value between zero and one, which represents a poor and good match, respectively.

Rock-physics models

Suitable rock-physics models for the regional gas sandstones and organic-rich shales are found by performing inverse rock-physics modeling based on density and acoustic well logs. This process involves matching petrophysical well logs and IRPM solutions by looping through various models and parameters. A rock-physics model was calibrated based on porosity, clay-content, and fluid-saturation logs through the well that penetrated the gas-sandstone reservoirs, resulting in a modified differential effective-medium model (DEM) with critical porosity constraints. The DEM model is an inclusion-based theory in which one constituent is considered the host medium, whereas the remaining components are embedded as inclusions. In the gas-sandstone model, mineral properties represent the host medium, whereas the elastic moduli of loose sands at critical porosity constitute inclusions (Mavko et al., 2009).

The rock-physics modeling for the organic-rich shale is more complicated and is shown schematically in Figure 3. Here, mixtures of kerogen, oil, and gas represent organic (Figure 3a), whereas clay, quartz, and feldspar are siliciclastic matter (Figure 3b), in a two-layer composite that can be represented as an effective medium using the Backus average (Figure 3c). In this study, we consider only normal-bedding properties in the Backus average. The kerogen maturation level is expressed by the volume of oil and gas within the solid kerogen. The organic and siliciclastic constituent properties are defined by probability distribution functions to infer uncertainties. A DEM model is then used to introduce shale porosity filled with brine (Figure 3d). For the model calibration, only data about the kerogen content from geochemical analysis in the wells penetrating the organic-rich shales were available.

Figure 4 shows IRPM-estimated and reported kerogen-to-siliciclastic volume fractions (i.e., kerogen content) represented by the colored dots and black lines, respectively, when using the final organic shale model. The reported kerogen is estimated from an empirical TOC-to-kerogen relation. The gray-to-red color gradient denotes the model probability and shows high values with a good match to the reported kerogen content at about 20% to 30%. From sensitivity testing of the two models, we also expect them to be applicable at intrawell anomalies, despite the depth difference.

A file with the details for the two rock-physics models is available as a downloadable XML file. Specifications of model parameters and other information required to reproduce our models can be found there.

Application to Norwegian Sea data set

We consider sections of seismically inverted acoustic impedance and P-to-S velocity ratio (V_P/V_S) from the Norwegian Sea. Figure 5 shows the AI section where the vertical dashed purple lines denote calibration wells and the green line represents the interpreted base Cretaceous unconformity (BCU) horizon. Seismic subsections of interest are studied at three locations:

1) on a structural high, where a discovery well encountered two Middle Jurassic gas-sandstone reservoirs (green area) with excellent reservoir quality (Figure 5a)

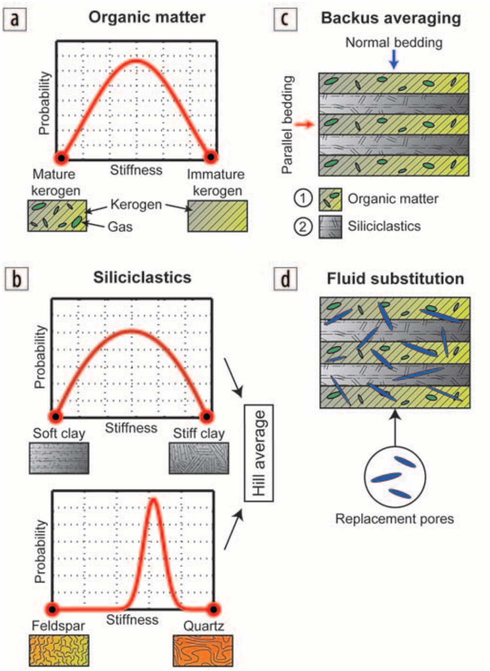

Figure 3. Rock-physics modeling of organic-rich shale represented as a four-step procedure. Parts (a) and (b) show probability distributions estimated for the various constituent properties; (c) and (d) show principal sketches of the Backus average and fluid substitution, respectively.

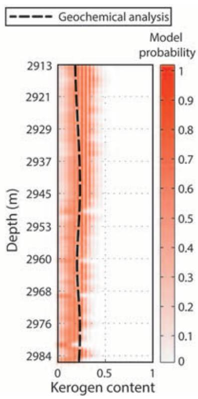

Figure 4. IRPM-estimated kerogen content from well-log measurements using the rock-physics model for the organic shale. The color bar denotes the model probability, and the dashed black line represents the reported kerogen content. Zero kerogen implies normal shales.

2) on a graben terrace downflank of a structural high, where a well penetrated a thick Upper Jurassic organic-rich shale (purple area) (Figure 5b)
3) in the graben between those two locations, where we suspect seismic anomalies right below the BCU to represent either gas sandstones or organic-rich shales (Figure 5c)

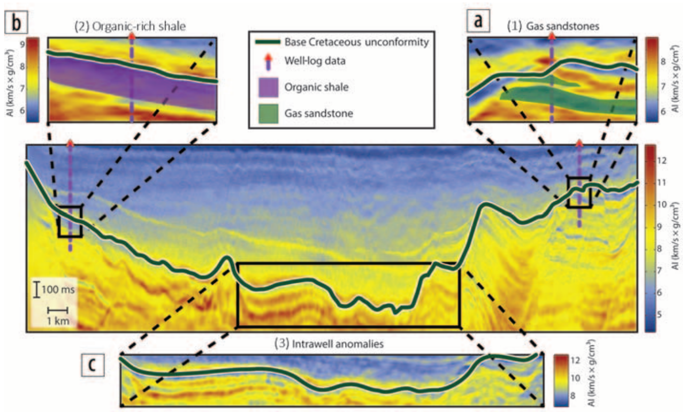

Figure 5. Section of acoustic impedance intersecting two wells (dashed purple lines) and the interpreted base Cretaceous unconformity horizon (green line). Three subsections (1, 2, and 3) represent (a) gas discovery (green area), (b) proven organic-rich shale (purple area), and (c) an intrawell anomaly.

To perform facies identification as described previously, the gas sandstone is specified by 10% to 40% porosity, 0% to 40% clay content, and 60% to 100% gas saturation, whereas the organic-rich shale is specified by 10% to 40% kerogen content.

To verify the performance of our calibrated rock-physics models, we apply our method to subsections 1 and 2 listed above (Figures 5a and 5b), where we have a good understanding of the local geologic and petrophysical conditions.

Figure 6 shows the facies identification based on the organic-rich shale model along with the gamma-ray and saturation well logs. The facies identifier in Figure 6a shows values close to zero in the gas-sandstone reservoir, implying that it is unlikely that this unit represents organic-rich shale. On the other hand, values close to one are obtained within the organic-rich shale unit in Figure 6b.

When testing the gas-sandstone model on the same data set, we achieved the opposite predictions. Hence, each model gave high likelihood for its respective facies in the units it is supposed to match and low likelihood for the other unit.

After having verified the two rock-physics models, we can proceed with the rock characterization. Figure 7 shows an example of the weighted mean and standard deviation of the predicted kerogen content based on the organic-rich shale model for subsection 2 (Figure 5b). The unit of organic-rich shale is outlined by the textured area with weighted-mean values of about 15% to 30% and standard deviation of 6% to 12%. Note that we should focus on the areas with high facies identification value (Figure 6b) because the predictions for the other areas are not reliable. Likewise, the weighted means from using the gas-sandstone model within the reservoir unit gave high porosities, low clay content, and high gas saturations, consistent with well-log observations.

Finally, Figures 8a and 8b show the facies identification based on the models for organic-rich shale and gas sandstone, respectively, for subsection 3 (Figure 5c). Along the whole section, the probability of organic-rich shale is quite low in the Upper Jurassic section, which is just beneath the BCU horizon (Figure 8a). In fact, in many places, we see white regions when using the organic-rich shale model, which means that the probability for the specified facies for this model falls below a minimum threshold, and we consider it as having no solutions.

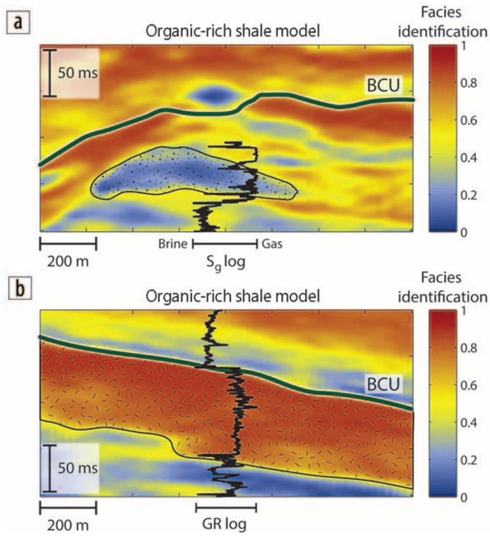

Figure 6. Facies identification based on the organic-rich shale model for subsections 1 and 2 (Figure 5a and 5b), respectively. The superimposed logs imply high gas saturations within the discovered reservoirs (dotted area) and high gamma ray within the proven organic-rich shale unit (textured area).

However, we see a high probability of gas sandstone just beneath the BCU horizon in the center of the section (Figure 8b). Hence, we assume that the observed seismic anomaly at this location represents a gas sandstone. Subsequently, we estimated weighted mean and standard deviation of reservoir properties, showing about 15% porosity, low clay content, and high gas saturation.

Discussion

We have performed facies identification and rock characterization from seismic-inversion data focusing on a Jurassic interval in the Norwegian Sea. For this, we used one rock-physics model calibrated to a gas-sandstone reservoir penetrated by a well and another model calibrated to an organic-rich shale penetrated by another well nearby. The two distinctive models gave good contrasts, making them suitable for facies identification. However, the performance of our approach depends on several factors that interpreters should be aware of, and some of these are discussed in this section.

The available well-log data penetrating the organic-rich shale (named Spekk Formation) lacks important petrophysical information, making an accurate model calibration more difficult. Moreover, limited research is performed on the rock physics of organic-rich shales, and the relationship between seismic properties and geologic variations is not fully understood. Hence, the organic-rich shale model is associated with large uncertainties and is probably not robust enough for accurate quantitative characterizations, as attempted in Figure 7. It still could be useful, however, for quick facies screenings and to obtain reliable trends.

The Spekk Formation is also studied by Løseth et al. (2011) in terms of total organic content estimates from seismic data. Similar to our results in Figure 7, Løseth et al. (2011) predict an upward-increasing TOC within the Spekk facies.

The isotropic Gassmann model often is used for fluid substitutions. However, its application for organic-rich shales fails because the assumptions of isotropic conditions and connected pores are disobeyed. Hence, we instead use a DEM model to introduce brine-filled inclusions. However, the elastic moduli are sensitive to the geometric details of the inclusions, which can be challenging to specify in the calibration procedure with deficient petrophysical data.

Furthermore, organic-rich shales have two pore systems — pores formed during sediment deposition and those formed later when hydrocarbons are expelled from the kerogen. Although we model pure brine saturations within the original shale porosity, it might be mixed with hydrocarbons leaked from the second pore system if the kerogen is sufficiently mature.

The organic-rich shale model used in this article considers only variations in the original shale porosity, whereas we infer uncertainties to the amount of expelled hydrocarbons. This is achieved by expressing the organic constituent properties by probability distribution functions via an average and standard deviation of immature and mature kerogen conditions. However, since the maturation level is not well known in the graben area, several models with different distribution functions should be evaluated.

To make predictions of kerogen maturation also, we varied the internal kerogen porosity from the expelled hydrocarbons. Both oil- and gas-bearing pores were considered, where gas represents more mature conditions than oil. Nevertheless, our predictions showed that it could not be differentiated; solutions were found for all possible maturation levels.

We have modeled isotropic rocks even though organic-rich shales often show very strong anisotropy. Consequently, our rock-physics model is possibly inadequate to describe the elastic moduli of organic-rich shales, which is potentially one explanation why we obtain so few solutions in Figure 8a. However, we also tested the parallel-bedding properties in the Backus average for the organic-rich shale model. The corresponding solutions were less convincing than when using the normal-bedding properties. This is reasonable when considering well-log data because the measurements are oriented normal to horizontal layering.

Seismic data, however, consist of multiple reflection events with varying angles of incidence, although most of the recorded events are closer to normal incidence. Hence, the normal-bedding properties seem reasonable. However, the probability distributions expressing the constituent properties might somehow include anisotropy effects.

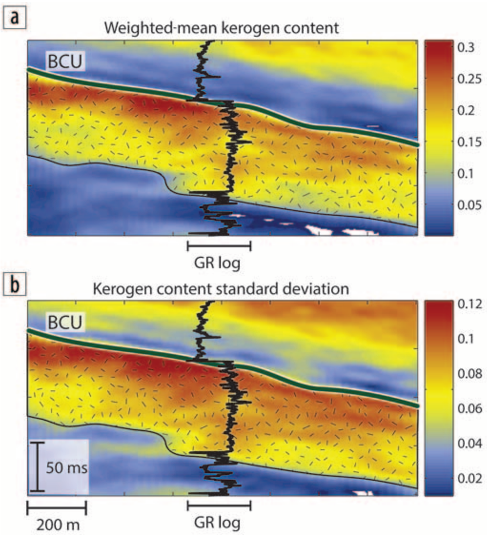

Figure 7. (a) Weighted mean and (b) standard deviation of kerogen content from subsection 2 (Figure 5b), based on the rock-physics model for the organic-rich shale.

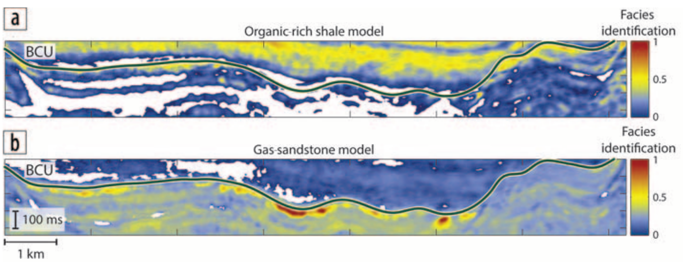

Figure 8. Facies identification within subsection 3 (Figure 5c), based on the rock-physics models for (a) organic-rich shale and (b) gas sandstone.

The seismically inverted data available for this study included seismic sections of AI and V_P/V_S. However, the great geologic variability and complexity of organic-rich shales can give a wide range of possible seismic properties which can overlap those typical of gas sandstones. Hence, additional geophysical observables might be required to distinguish these rocks from one another and to better constrain the nonunique solutions. Another issue is that the seismic-inversion data in the graben area become more uncertain with distance from well locations. Adding some relative uncertainty to the input data will address this, but the actual amount and influence of seismic uncertainties are difficult to implement.

Conclusions

We have shown how we can use inverse rock-physics modeling to screen for organic-rich shales and gas sandstones when seismic-inversion data are available. Our method allows us to implement model and data uncertainties and to investigate the nonuniqueness of solutions consistent with rock-physics models. We demonstrate the method on a data set from the Norwegian Sea focusing on an Upper Jurassic interval with some interesting seismic anomalies. Two rock-physics models were calibrated from regional well-log data, one model for organic-rich shales and another for gas sandstones. Our predictions imply that presence of organic-rich shales is more unlikely than gas sandstones for the observed seismic anomalies. However, predictions in frontier basins are uncertain as we move outside the range of well control where our models and seismic-inversion data cannot be validated. Hence, our seismic screening should be evaluated in conjunction with other geologic and geophysical information to reduce interpretation risk. TLE

Acknowledgments

We thank Tullow Oil for sharing data and useful input. We would also like to thank Tullow Oil, Christian Michelsen Research, and Statoil for financing the Ph.D. program of Kenneth Bredesen.

Corresponding author: Kenneth.Bredesen@uib.no

References

Avseth, P., T. Veggeland, and F. Horn, 2014, Seismic screening for hydrocarbon prospects using rock-physics attributes: The Leading Edge, **33**, no. 3, 266–274, http://dx.doi.org/10.1190/tle33030266.1.

Johansen, T. A., E. H. Jensen, G. Mavko, and J. Dvorkin, 2013, Inverse rock physics modeling for reservoir quality prediction: Geophysics, **78**, no. 2, M1–M18, http://dx.doi.org/10.1190/geo2012-0215.1.

Khadeeva, Y., and L. Vernik, 2014, Rock-physics model for unconventional shales: The Leading Edge, **33**, no. 3, 318–322, http://dx.doi.org/10.1190/tle33030318.1.

Løseth, H., L. Wensaas, M. Gading, K. Duffaut, and M. Springer, 2011, Can hydrocarbon source rocks be identified on seismic data?: Geology, **39**, no. 12, 1167–1170, http://dx.doi.org/10.1130/G32328.1.

Mavko, G., T. Mukerji, and J. Dvorkin, 2009, The rock physics handbook: Tools for seismic analysis of porous media, 2nd ed.: Cambridge University Press, http://dx.doi.org/10.1017/CBO9780511626753.